A High-Q Reconfigurable Planar EBG Cavity Resonator

Michael J. Hill, Richard W. Ziolkowski, and John Papapolymerou

***Abstract*—A reconfigurable planar electromagnetic bandgap (EBG) cavity resonator has been designed, fabricated, and tested. The resonator, based on a microstrip-coupled cavity constructed with periodic metallic post side walls, resonates at 10.60 GHz or 8.63 GHz, depending on the state of two rows of switchable post elements. Fabricated on 0.031" 5880 Duroid, the resonator exhibits Qs of 448 and 274 for the 10.60-GHz and 8.63-GHz resonances, respectively. In addition to the reasonably high Qs achievable with this design, the circuit utilizes standard printed circuit board (PCB) fabrication techniques and is 100% compatible with commercial PCB processes, enabling low-cost mass production.**

I. Introduction

ELECTROMAGNETIC bandgap (EBG) structures have received much interest recently. Although there is much debate over terminology with respect to these structures [1], EBGs typically consist of periodic arrangements of metallic or dielectric elements forming a structure that alters the allowed modes of electromagnetic propagation [2]. With proper design, an EBG structure can be used to define the side walls of a resonant cavity [3]. This EBG cavity can then replace the fully conducting side wall (FCSW) cavity in a microstrip-coupled resonator [4]. There are two distinct advantages that this configuration has over the FCSW configuration. First, the EBG cavity allows for reconfigurability through the switching of one or more of the posts defining the cavity wall. This switching can be mechanical or electrical. Second, the EBG cavity can be constructed using printed circuit board (PCB) techniques in an inexpensive Duroid substrate. This eliminates the costly machining required to produce a FCSW cavity, reduces the difficulties associated with the bonding of the feed circuit and cavity lid to the machined FCSW cavity structure, and allows for inexpensive mass production.

II. Circuit Design and Topology

The reconfigurable EBG resonator is based on the microstrip coupled EBG resonator [3] shown in Fig. 1. This circuit utilizes two magnetic coupling slots in the ground plane of a microstrip feed line to couple energy into the resonant cavity defined by the EBG cavity walls. The resonant frequency of the TE_{101} cavity mode is well approximated by

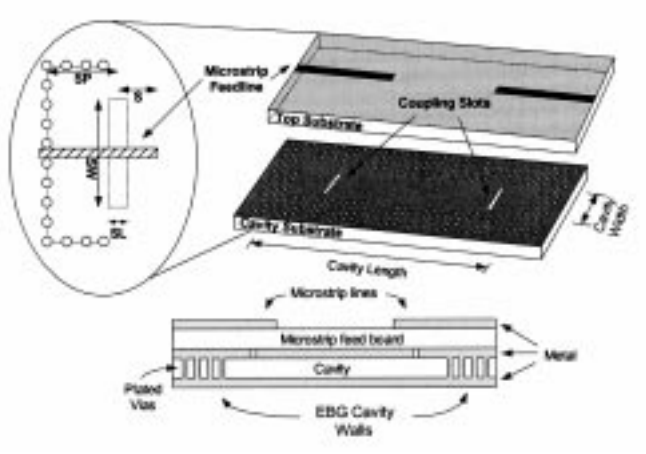

Fig. 1. Microstrip coupled EBG cavity resonator.

$$f_{\mathrm{res}} = \frac{c}{2\pi\sqrt{\varepsilon_r}}\sqrt{\left(\frac{\pi}{L}\right)^2 + \left(\frac{\pi}{W}\right)^2} \tag{1}$$

where L and W are the effective length and width of the cavity.

Typically, the coupling slots are located approximately $L/4$ from the edge of the cavity (SP of Fig. 1) and are designed according to the procedure outlined in [4]. For efficient coupling to the microstrip lines, an electric short circuit should exist at the center of the coupling slot. In a single frequency resonator, this is often produced with an open-circuited stub that extends $\lambda/4$ beyond the slot center (S of Fig. 1). For a reconfigurable resonator that operates at two or more frequencies, a shorting via must be used in place of the quarter wave open-circuited stub to provide the short at the coupling slot at all resonant frequencies.

In order to provide reconfigurability, special switchable post elements are introduced at two of the cavity side walls. By turning these posts "on" the effective width of the cavity is reduced, thereby increasing the resonant frequency of the circuit (see Fig. 2). In the circuit presented here, one row on each side of the cavity was created with switchable elements, but more than one row could be "switched" and would allow the operation of more than two resonant frequencies.

The switchable and static elements used in the EBG walls of this cavity are constructed using metalized vias. In order to create a switchable element from a standard via, an annular ring was used to electrically disconnect the top of the via from the ground plane closing the top of the cavity structure (see Fig. 3). By removing the current path connecting the via post to the top

Manuscript received January 22, 2001; revised April 23, 2001. This work was supported in part by the Air Force Office of Scientific Research, Air Force Material Command, USAF, under Grant F49620-96-1-0039 and by the NSF-S/IUCRC Center for Low Power Electronics (CLPE) under Grant EEC-9523338. The review of this letter was arranged by Associate Editor Dr. Ruediger Vahldieck.

The authors are with the Department of Electrical and Computer Engineering, The University of Arizona, Tucson, AZ 85721 USA.

Publisher Item Identifier S 1531-1309(01)05429-0.

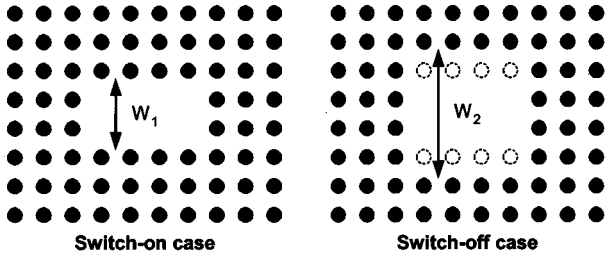

Fig. 2. Reconfigurable cavity wall.

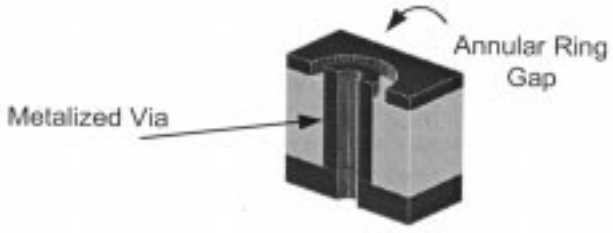

Fig. 3. Switchable via element.

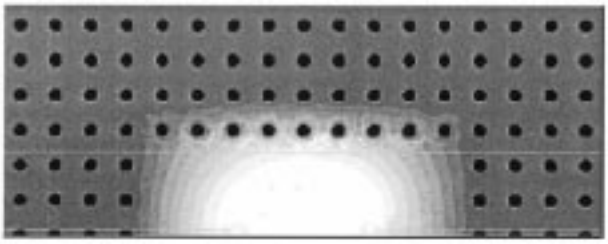

Fig. 4. HFSS cavity field plot (half cavity), switch-off case.

of the cavity, the blocking effect of the post is essentially removed (see Fig. 4). When assembled, the ground plane of the top board does not extend over the annular rings, thus preventing the top board from closing the annular ring gap. In the current configuration the switching action is mechanical, but an electronic or MEMS switch version could be implemented.

The cavity circuit was constructed on 0.031" thick Rogers Duroid 5880 ($\epsilon_r = 2.2$). This material was chosen because of its low-loss tangent ($\tan\delta = 0.0009$). The feed board was fabricated on Rogers Duroid 6010 ($\epsilon_r = 10.8$), although other materials could be used with appropriate adjustment of the feed line widths. Using the methods outlined in [3] and [4], the design parameters shown in Table I (refer to Fig. 1) were chosen. The EBG used utilized four rows of vias (including the switchable row) to define the cavity walls (see Fig. 1).

III. Simulation and Measurement

The reconfigurable resonator structure was simulated using Ansoft's high-frequency structure simulator (HFSS). Simulations were run for the switch-on and switch-off cases. In both cases, the coupling slots were adjusted to provide low-cavity coupling. This enabled the unloaded quality factor ($Q_{\rm U}$) to be extracted from the simulation data. Because the simulated $Q_{\rm U}$ must be extracted using low-coupling data, the results can be impacted by both the dynamic range of the simulations and the

TABLE I
Design Parameters

SP	5.26 mm	Cavity Length	18.9 mm
SW	2.30 mm	Cavity Width	
SL	0.14 mm	Switch On	11.34 mm
Via Diameter	0.79 mm	Switch Off	15.12 mm
Via Spacing	1.89 mm		

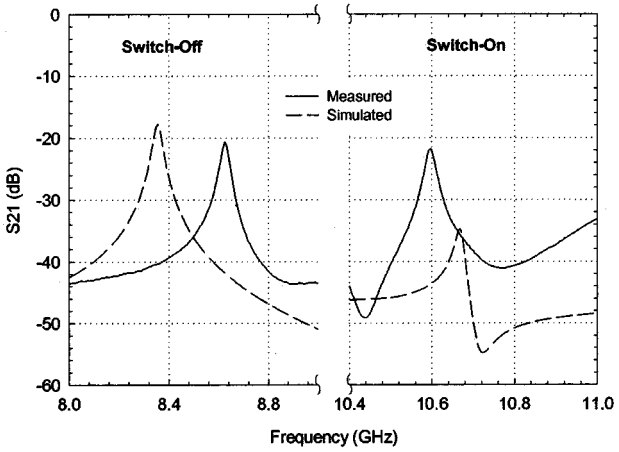

Fig. 5. Measured and simulated results.

TABLE II
Simulated and Measured Results

Switch state	Resonant Freq.	Unloaded Q
On – simulated	10.67 GHz	445
On – measured	10.60 GHz	448
Off – simulated	8.36 GHz	260
Off – measured	8.63 GHz	274

simulation mesh. To ensure an accurate result, multiple simulations were run; the results were compared to each other and to simulations performed using the HFSS eigenmode solver. The quality factor was then calculated using (2)–(4), [4]

$$Q_{\rm loaded} = \frac{f_o}{\Delta f} \tag{2}$$

$$Q_{\rm external} = 10^{-[S_{21}({\rm dB})/20]} \cdot Q_{\rm loaded} \tag{3}$$

$$Q_{\rm U}^{-1} = Q_{\rm loaded}^{-1} - Q_{\rm external}^{-1}. \tag{4}$$

The simulated and measured results for the switch-on and switch-off cases are shown in Fig. 5. Table II summarizes the numerical results of the simulations and measurements. Generally, the measured and simulated results agree well (0.67% difference in resonant frequency for the switch-on case and 3.1% difference for the switch-off case). There is some discrepancy between the measured and simulated results for the resonant frequency of the switch-off case. The resonant frequency of the switch-off case can be affected by the capacitance between the top of the post and the cavity lid. This capacitance is a function of the annular ring design and construction. Although this capacitance is included in the full-wave simulations, the vias were modeled as octagonal rather than cylindrical posts. This

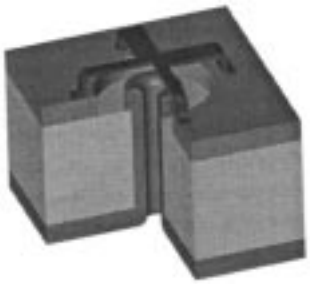

Fig. 6. Improved switch element, off state.

allowed reasonable-sized simulation meshes, but may have introduced some inaccuracy in the modeling, and, therefore, may have contributed to the discrepancy between simulated and measured results. Additionally, it is likely that inaccuracies in the manual drilling of the vias introduced some error.

From this data, it is clear that the switch-off case exhibits significantly lower Q than the switch-on case. This was investigated and it was found that the annular nonconducting ring forming the switchable element was introducing additional metal losses in the cavity lid. To circumvent this problem, the structure of Fig. 6 was simulated. This structure allows currents on the top of the cavity to pass over the open switched via, and reduces the current density around the edge of the annular ring. Simulation results from this case indicate Q_{U}s much closer to those of the switch-on case. Because of the difficulty in constructing this "cap," this concept has not yet been fabricated. Because the topology of this "cap" is similar to a MEMS switch, MEMS-like devices could be used to implement both this "cap" and electronic switching of the post element. Additionally, a similar structure could be used to introduce a variable capacitance between the post and cavity lid. This could enable continuous adjustment of the resonant frequency between the two discrete states of the current device. A similar effect may be possible by switching individual posts, rather than complete rows of posts. This would provide multiple discrete resonances to approximate a continuous adjustment.

IV. Conclusion

A reconfigurable high-Q, planar resonator has been designed, fabricated, and tested. Because the resonator utilizes planar construction and microstrip feeds, it is easy to integrate with other planar circuits. Additionally, the resonator is compatible with standard printed circuit board printing techniques. This, coupled with the ability to reconfigure the resonant frequency, makes the circuit well suited for use in mass produced, cost-sensitive microwave devices.

Future work will enhance the current design. Because the cavity Q is highly dependent on the cavity board thickness [3], simulations have shown that future designs with thicker cavity substrates will result in resonators with Q's above 500. Work will also focus on implementing an electronically-controllable switching element, as well as implementing the "cap" of Fig. 6. Professional fabrication will be utilized to enhance fabrication accuracy and the correlation between simulation and measurement. Using these resonators, reconfigurable controlled ripple filters will be designed and tested.

Acknowledgment

The authors would also like to thank Rogers Corporation for supplying the substrate material.

References

[1] A. Oliner, "Periodic structures and photinic-band-gap terminology: historical perspectives," in *Proc. 29th Eur. Microw. Conf.*, vol. 3, Munich, Germany, Oct. 1999, pp. 295–298.

[2] J. D. Joannopoulos, *Photonic Crystals: Molding the Flow of Light.* Princeton, N.J.: Princeton Univ. Press, 1995.

[3] M. J. Hill, R. W. Ziolkowski, and J. Papapolymerou, "Simulated and measured results from a Duroid-based planar MBG cavity resonator filter," *IEEE Microwave Guided Wave Lett.*, vol. 10, pp. 528–530, Dec. 2000.

[4] J. Papapolymerou, J. Cheng, J. East, and L. Katehi, "A micromachined high-Q X-band resonator," *IEEE Microw. Guided Wave Lett.*, vol. 7, pp. 168–170, June 1997.